

DIFFRACTION AND SCATTERING OF IONIZING RADIATIONS

Observation of Strong Virtual Scattering under Three-Beam (220, 371) X-Ray Diffraction in TeO₂ Single Crystal

A. E. Blagov^a, M. V. Kovalchuk^{a, b}, V. G. Kohn^b, Yu. V. Pisarevskii^a, and P. A. Prosekov^a

^a Shubnikov Institute of Crystallography, Russian Academy of Sciences, Leninskii pr. 59, Moscow, 119333 Russia

e-mail: aopt@ns.crys.ras.ru

^b Russian Research Centre, Kurchatov Institute, pl. Akademika Kurchatova 1, Moscow, 123182 Russia

Received June 10, 2009

Abstract—A strong effect of virtual scattering has been experimentally observed when studying the nearly coplanar three-beam (220, 371) X-ray diffraction in a paratellurite single crystal under high-resolution double-crystal X-ray diffraction using MoK_{α1} radiation. One characteristic feature of this effect is that the angular dependence of the first (strong) reflection intensity and its shape barely change in the three-beam range of parameters, whereas very strong changes are observed for the second (weak) reflection not only in the three-beam range but also far beyond it, which is related to the variation in the two-beam diffraction parameter due to virtual scattering. The changes observed are asymmetric and make it possible to determine the triplet combination of structure-factor phases.

DOI: 10.1134/S1063774510010037

INTRODUCTION

The experimental scheme of high-resolution X-ray diffraction with a laboratory source can be used to study multibeam diffraction effects [1]. Interesting results have been obtained for the coplanar three-beam diffraction [2, 3], in which the reflections from two systems of atomic planes occur in the same scattering plane; i.e., the directions of the incident and two diffracted beams lie in the same plane.

Generally the radiation wave function is significantly transformed into the three-beam range of parameters, where the Bragg conditions for two reflections of the same intensity are simultaneously satisfied. However, if the first reflection is strong but the second reflection is weak, an asymmetric situation arises. The strong reflection almost does not change in the three-beam region, whereas the weak reflection characteristically changes. In the range of total diffraction into the first (strong) reflection, this perturbation shows typical dispersion behavior (enhancement at one side and reduction at the other side; see, for example, [2, 3]). This type of scattering was referred to as amplitude scattering in [4]. It was also shown in [4] that there is another scattering process: resonant or virtual scattering, where the first-reflection beam is very weak because the Bragg conditions are satisfied only approximately and the change in the second reflection is significant and occurs in a very wide range of the parameter, determining the deviation from the Bragg condition for the first reflection.

In this paper we report the results of the first experimental observation of the virtual scattering effect in a

study of the nearly coplanar three-beam (220, 371) X-ray diffraction in a paratellurite (TeO₂) single crystal in the scheme of high-resolution double-crystal X-ray diffraction using MoK_{α1} radiation.

A schematic of the experiment is shown in Fig. 1. The radiation from the X-ray tube anode is collimated by the monochromator and directed to the sample. The slit on the beam path makes it possible to select one line in the spectrum of characteristic K_{α1} and K_{α2} doublet. The two beams emerging from the sample are simultaneously recorded by two detectors, and the intensity dependence upon crystal rocking in the scattering plane (polar scanning over small angle θ_2) is measured. The crystal rotation in the plane perpendicular to the scattering plane, for example, around the reciprocal lattice vector for the first reflection (azi-

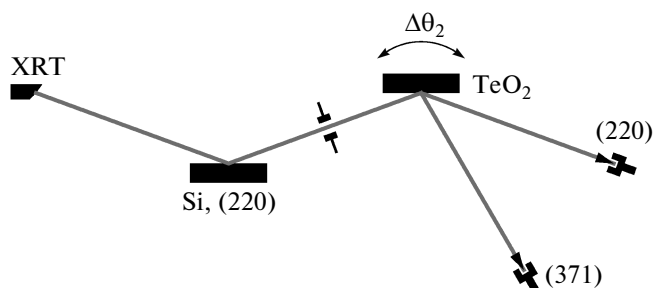


Fig. 1. Schematic of the experiment: X-ray tube (XRT), silicon monochromator (Si, (220)), and TeO₂ sample. Two reflections are recorded by two detectors.

azimuthal rotation by a relatively large angle θ_1), makes it possible to set any degree of deviation from the multibeam orientation for the maximum in the spectrum or, vice versa, to orient the crystal into the multibeam angular position if the spectral maximum does not exactly correspond to coplanar diffraction.

One important circumstance is that the relative width of the spectral characteristic line exceeds the angular range of dynamic diffraction in the single crystal by a factor of more than 10. Nondispersive or weakly dispersive scattering can be provided only for the first reflection. For the second reflection, the angular intensity dependence is significantly broadened due to the integration over the width of the spectral line used, whereas the intensity of the second reflection is several tens of times lower than that of the first one. It is this weak reflection that makes it possible to record multibeam diffraction, in particular, to determine the triplet phase combination for the structural amplitudes of the reflections under consideration [5].

The dispersive character of the angular dependence of the second reflection in the range of strong scattering into the first reflection is explained as follows: the second reflection is formed by a coherent superposition of the incident and first reflected plane waves; the phase difference between them runs from 0 to π upon passage through the first-reflection dynamic range. This situation is similar to that in the X-ray standing wave method, and the weak reflection plays the role of secondary radiation [6].

Virtual scattering occurs in the range of weak diffraction into the first reflection. It is one of the most beautiful effects of multibeam diffraction. It was experimentally studied in [7, 8] using the low-resolution Renninger scheme, where the dependence of the polar-angle integrated intensity on the azimuthal angle is recorded. The essence of the virtual scattering theory [9] is that the diffraction reflection of the second wave remains a two-wave one, but the diffraction parameters change due to the weak (virtual) scattering by the first wave. The necessary conditions for observing this effect are as follows: the first reflection must be sufficiently strong and the second reflection must be weak or even forbidden [4].

In this study we chose the strong (220) reflection and weak (371) reflection in a TeO_2 single crystal. The coplanar diffraction for this pair occurs at a radiation wavelength that is fairly close to that of the $\text{Mo}K_{\alpha 1}$ line but does not exactly coincide with it. Therefore, to study the multibeam effects, we had to withdraw the crystal from the exact coplanar position so as to prevent the diffraction character from significant variations.

THEORY AND COMPUTER SIMULATION

To clarify the experimental data, let us first consider the results of a computer simulation of the angular dependences of reflections in this scheme. The TeO_2 crystal has a tetragonal unit cell composed of four molecules. The lattice parameters for calculating the structure factors were taken from [10]: $a = b = 4.810 \text{ \AA}$ and $c = 7.613 \text{ \AA}$. This crystal was also studied in [11], where the lattice parameters were found to have very close values. Accordingly, the three-beam coplanar (220), (371) diffraction occurs at the wavelength $\lambda_0 = 0.71006 \text{ \AA}$. This value only slightly exceeds the wavelength of the $\text{Mo}K_{\alpha 1}$ line (0.70932 \AA). Since the wavelengths cannot be changed in the experiment, the crystal was set into the multibeam position by azimuthal rotation in a narrow range. Changing the angle of rotation, one can provide any degree of multibeam diffraction mismatch. In the theoretical calculations it was assumed for simplicity that the coplanar case is satisfied exactly, and the multibeam diffraction mismatch is provided by varying the wavelength. At rotations by small azimuthal angles and small variations in the wavelength, these two approaches differ only slightly.

In the coplanar case, the reflection intensity is independent of the angle θ_1 but depends on the wavelength variation $\Delta\lambda$. It is convenient to introduce the third small angle: $\theta_3 = -\Delta\lambda/\lambda_0$. In the high-resolution X-ray diffraction method, one generally uses the plane-wave approach to theoretically analyze the results. Within this approach the X-ray beam that is incident on the crystal is approximated by a set of incoherent plane waves; each of them is characterized by three parameters $(\theta_1, \theta_2, \theta_3)$. It is necessary to solve the problem of three-beam diffraction for each plane wave of this set and then integrate the reflected beam intensities over these three parameters with a required weight and in the specified limits. Since (i) the reflection intensities are independent of the angle θ_1 when the latter is small and (ii) the integration limits are determined by the entrance slit, the integration over this angle is equivalent to multiplication by a constant factor. The integration over θ_3 must be performed with a weight function describing the shape of the X-ray tube line spectrum. The calculations were performed using the Lorentz function with a half-width of $340 \mu\text{rad}$ centered at the point $\Delta\theta_3$. In this case, the zero value of $\Delta\theta_3$ corresponded to the wavelength λ_0 . The limits of integration over θ_2 are set by the monochromator; in this case it is sufficient to take into account only the total reflection range of the monochromator.

We calculated the dependences of the intensity on the angular mismatch $\Delta\theta_2$ between the monochromator and the sample. Varying the parameter $\Delta\theta_3$, we obtained a series of curves describing the three-beam diffraction decomposition into two independent cases

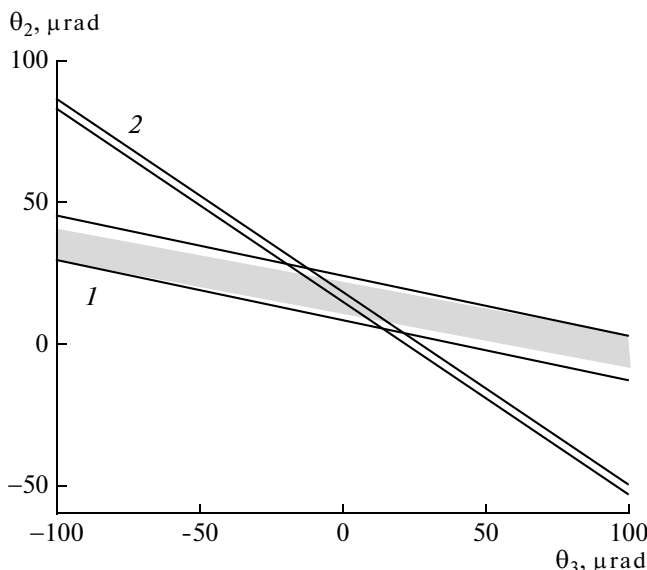


Fig. 2. Diagram indicating the position of the two-beam ranges of total reflection in the plane of parameters (relative photon energy, polar angle): (220) reflection band (1) and (371) reflection band (2). The gray area corresponds to the strong reflection from the monochromator.

of two-beam diffraction. Using the Du Mond diagram [12] (Fig. 2), one can determine the integration limits and integrand character. The two-wave diffraction conditions are known to occur along the band parallel to the $\theta_2 = -\theta_3 \tan(\theta_B)$ line, where θ_B is the Bragg angle. The width of this band is proportional to the diffraction parameter, which is equal to the Fourier component of the crystal polarizability for a specified reciprocal lattice vector. This experiment was performed using a silicon monochromator and a symmetric (220) reflection ($\theta_B = 10.645^\circ$). The angular width of this reflection is 10 μrad. The Bragg angles for the (220) and (371) reflections in paratellurite are 12.037° and 34.292°, respectively. The (220) reflection is also symmetric, whereas the angle between the beam and crystal surface for the (371) reflection is 56.547°.

Figure 2 shows (in gray) the total reflection range for the monochromator over which the integration is performed. The limits of the total reflection ranges for the (220) (wide) and (371) (narrow) reflections are also indicated. It can be seen that, at the angle $\Delta\theta_2$ corresponding to the peak centroid for the first reflection, the range of integration almost completely lies in the strong reflection band and rapidly leaves it with a change in this angle. At the same time, the range of integration crosses the weak reflection band only at a small portion at all values of $\Delta\theta_2$. One important circumstance is that the angular dependence of the reflection intensity (even an approximate one) can be obtained only for the first reflection, for which the Bragg angle is close to that of the monochromator. It is the angle-integrated intensity that is constantly

recorded for the second reflection; its value is proportional to the incident-beam intensity at the wavelength corresponding to the intersection of the monochromator and second-reflection bands. If the emission spectrum is approximated by a Lorentzian function, the second-reflection peak has also a Lorentzian shape for the curves where the multibeam diffraction is insignificant.

The three-beam diffraction for an incident plane wave was calculated according to the standard algorithm, which was described for the first time in [13]. We first calculated a 2D map of the dependence on θ_2 and θ_3 at a specified value of $\Delta\theta_3$ and then performed summation over the band cut by the monochromator at different angular mismatches $\Delta\theta_2$. The calculation results are shown in Fig. 3. All the angles are in microradians. The intensity of the strong beam (narrow peak) is normalized to unity, while the intensity of the weak beam (wide peak) is multiplied by 50 to make the curves fall in the same range. Due to small difference in the Bragg angles for the monochromator and first reflection, the peak corresponding to the latter is slightly broadened. The range for the second reflection (371), as was noted above, sets the shape of the characteristic line spectrum. The angular distance between the centers of the two peaks (obtained by subtracting the second peak from the first one) is given by the formula

$$\Delta\theta_{2d} = \Delta\theta_3 (\tan\theta_{B1} - \tan\theta_{B2}). \quad (1)$$

The peak positions are given taking into account the shift caused by the refraction in the crystal.

As follows from the calculations, the weak reflection intensity changes significantly not only in the three-beam range but also beyond it (where the contribution to the strong reflection is very small). In the 2D maps one can clearly see that the reflection is nearly two-wave in these ranges, but the total reflection band is wider than in the two-wave case at the one side and smaller at the other side. This fact directly indicates that the two-wave diffraction parameter changes due to the virtual scattering from the first reflection.

To illustrate the aforesaid, let us consider the simplest case of three-beam coplanar diffraction of a monochromatic plane wave polarized perpendicularly to the scattering plane. In this case, the complex amplitudes of the three waves, E_0 , E_1 , and E_2 , are found from the system of equations

$$\begin{aligned} \chi_{00}E_0 + \chi_{01}E_1 + \chi_{02}E_2 &= \gamma_0 \varepsilon E_0, \\ \chi_{10}E_0 + (\chi_{11} - \alpha_1)E_1 + \chi_{12}E_2 &= \gamma_1 \varepsilon E_1, \\ \chi_{20}E_0 + \chi_{21}E_1 + (\chi_{22} - \alpha_2)E_2 &= \gamma_2 \varepsilon E_2, \end{aligned} \quad (2)$$

where χ_{mn} is the Fourier component of the crystal complex polarizability at the reciprocal lattice vector $\mathbf{h}_m - \mathbf{h}_n$; α_1 and α_2 are the parameters of deviation from the Bragg condition for the two diffracted waves; γ_0 , γ_1 , and γ_2 are the cosines of the angles between the inner normal to the crystal surface and the three wave direc-

tions; and ε is the complex dispersion correction to the wave vectors, which takes into account the wave refraction at the crystal boundary and absorption in the crystal bulk.

For the parameter values at which the reflection into wave 2 is still fairly strong but the reflection into wave 1 is already weak, we have the inequality $\alpha_1 \gg \chi_{mn}$, ε . It is obvious that the second equation is solved only at a very small value of the amplitude E_1 , which is approximately

$$E_1 = \frac{\chi_{10}E_0 + \chi_{12}E_2}{\alpha_1}. \quad (3)$$

Substituting this value into (2), we obtain a system of two equations for the two-beam diffraction:

$$\begin{aligned} g_{00}E_0 + g_{02}E_2 &= \gamma_0\varepsilon E_0, \\ g_{20}E_0 + (g_{22} - \alpha_2)E_2 &= \gamma_2\varepsilon E_2, \end{aligned} \quad (4)$$

where

$$\begin{aligned} g_{00} &= \chi_{00} + \frac{\chi_{01}\chi_{10}}{\alpha_1}, & g_{02} &= \chi_{02} + \frac{\chi_{01}\chi_{12}}{\alpha_1}, \\ g_{20} &= \chi_{20} + \frac{\chi_{21}\chi_{10}}{\alpha_1}, & g_{22} &= \chi_{22} + \frac{\chi_{21}\chi_{12}}{\alpha_1}. \end{aligned} \quad (5)$$

The two-beam diffraction equations can be solved exactly. It is known that the integrated intensity is proportional to $|g_{02}g_{20}|^{1/2}$. Taking into account formulas (5), one can conclude that the integrated intensity depends on the triplet phase invariant $\varphi_{01} + \varphi_{12} - \varphi_{02}$, where φ_{mn} is the phase of the complex quantity χ_{mn} . In addition, it depends on the sign of the deviation from the Bragg condition. This is why the integrated intensity increases at one side and decreases at the other side in comparison with the pure two-beam case.

Using well-known geometric formulas [14] and the above-mentioned parameters, one can easily find that, under the conditions of three-beam diffraction for MoK_{α1} radiation, the second beam (371) should make the angle $\theta_g = 56.55^\circ$ with the crystal surface and the angle $\varphi_g = 1.14^\circ$ with the scattering plane for the first reflection (220). The azimuthal angle $\Delta\theta_1 = 2.67^\circ$ of crystal rotation from the coplanar geometry into the multibeam position is calculated from the formula

$$\tan(\Delta\theta_1) = \sin(\varphi_g)/[\cos(\theta_B) - \cos(\theta_g)\cos(\varphi_g)]. \quad (6)$$

At the same time, applying formula (1), we estimate the difference in the angular positions of the two peaks in the coplanar case at $\Delta\theta_3 = 1043 \mu\text{rad}$ to be $\Delta\theta_{2d} = -488 \mu\text{rad}$, a value nearly coinciding with the experimental data.

EXPERIMENTAL RESULTS AND DISCUSSION

Figure 4 shows a series of experimental curves for the transmission through the multibeam region obtained by varying the azimuthal angle by 10 arcmin. The upper plot corresponds to the crystal position

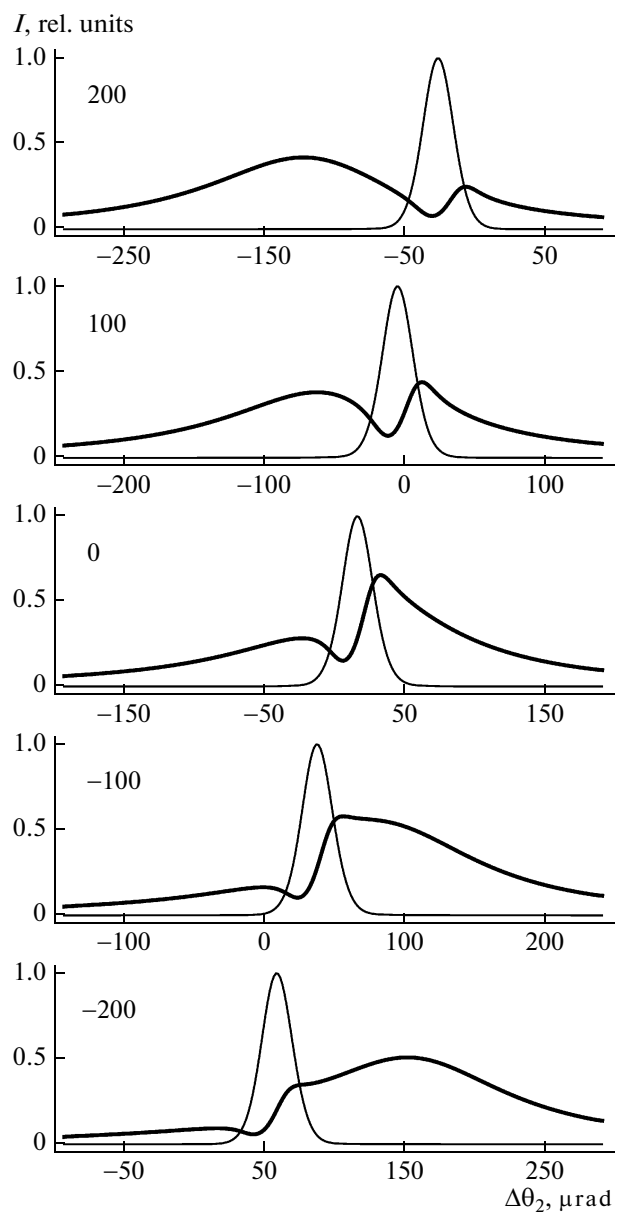


Fig. 3. Theoretical dependences of the reflection coefficients on the polar angle in the coplanar case at different energy shifts in the center of the spectral line described by a Lorentzian function and having a relative half-width of 340 μrad : (thin lines) (220) reflection and (bold lines) (371) reflection. The relative energy shifts (in μrad) with respect to the multibeam point are indicated.

close to coplanar. The curves for the strong reflection (220) are normalized to unity, while the curves for the weak reflection (371) are normalized so as to be noticeable in the figure. The normalization for all plots is the same; however, the absolute ratio of the intensities was not measured.

Comparing Figs. 3 and 4, one can easily make sure that the main features of changes in the curves are the same, despite the fact that the experimental condi-

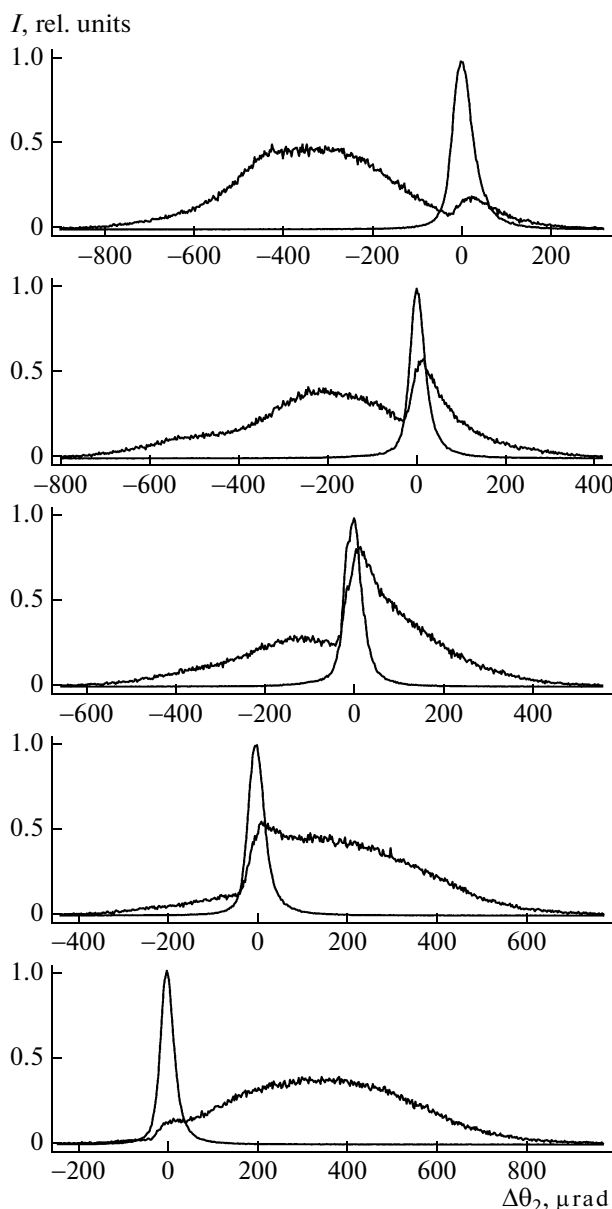


Fig. 4. Experimental dependences of the reflection coefficients on the polar angle at different values of the azimuthal angle over the multibeam range with a step of 10 arcmin.

tions differed from the strictly coplanar case and collimation over the azimuthal angle was not performed intentionally. This was only determined by the slits that were always present in the experiment. This is a likely reason for the deviation of the shape of the weak reflection peak from Lorentzian and for the slight excess of its width above that predicted by the theory. In addition, the upper curve contains pronounced artifacts (additional bendings of the weak reflection curve). These are likely to be caused by the insufficient structural quality of the paratellurite crystal. Note that the crystal surface was etched to a fairly large depth

before the measurements. The measurements of the curves prior to the etching showed a very significant increase in the reflection region even for the strong reflection. It is of interest that the multibeam interaction was well pronounced even for the unetched sample. However, these results cannot be compared with the theory because the latter has not been developed for distorted crystals; in addition, the character of crystal deformation was unknown.

The analysis of the multibeam phenomena in various single crystals of technical importance can be promising for studying their structure and degree of structural quality and obtaining more diverse data than two-beam diffraction. Here we investigated paratellurite crystals in the double-crystal scheme for the first time. The use of the triple-crystal scheme with two monochromator crystals will make it possible to obtain more detailed information.

ACKNOWLEDGMENTS

This study was supported by the Russian Foundation for Basic Research (project nos. 08-02-12078-ofi, 09-02-12164-ofi_m, and 07-02-00067a); grant 02.120.11.4830-MK of the President of the Russian Federation; and (in part) grant NSh-1955.2008.2 for Support of Leading Scientific Schools.

REFERENCES

1. É. K. Kov'ev and V. I. Simonov, Pis'ma Zh. Eksp. Teor. Fiz. **43**, 244 (1986) [JETP Lett. (Engl. Transl.), **43**, 312 (1986)].
2. A. M. Afanas'ev, A. V. Zozulya, M. V. Kovalchuk, and M. A. Chuev, Pis'ma Zh. Eksp. Teor. Fiz. **75**, 379 (2002) [JETP Lett. (Engl. Transl.), **75**, 309 (2002)].
3. A. V. Zozulya, M. V. Kovalchuk, V. V. Lider, and L. V. Samoilova, Poverkhnost **7**, 6 (2002).
4. V. G. Kohn, Kristallografiya **33**, 567 (1988) [Sov. Phys. Crystallogr. (Engl. Transl.), **33**, 333 (1988)].
5. S.-L. Chang, *Multiple Diffraction of X Rays in Crystals* (Berlin, Springer, 1984; Moscow, Mir, 1987).
6. V. G. Kohn, Phys. Status Solidi A **106**, 31 (1988).
7. L. D. Chapman, D. R. Yoder, and R. Colella, Phys. Rev. Lett. **46**, 1578 (1981).
8. M. C. Schmidt and R. Colella, Phys. Rev. Lett. **55**, 715 (1985).
9. R. Hoier and K. Martinsen, Acta Crystallogr. A **39**, 854 (1983).
10. I. P. Kondrat'ev, L. A. Muradyan, Yu. V. Pisarevskii, and V. I. Simonov, Kristallografiya **32**, 609 (1987) [Sov. Phys. Crystallogr. (Engl. Transl.), **32**, 354 (1987)].
11. P. A. Tomas, J. Phys. C: Solid State Phys. **21**, 4611 (1988).
12. Z. G. Pinsker, *X-ray Crystal Optics* (Nauka, Moscow, 1982) [in Russian].
13. V. G. Kohn, Phys. Status Solidi A **54**, 375 (1979).

Translated by Yu. Sin'kov